

Structural and photoluminescent properties of ZnO hexagonal nanoprisms synthesized by microemulsion with polyvinyl pyrrolidone served as surfactant and passivant

Xiaomeng Sui ^{a,b}, Yichun Liu ^{c,*}, Changlu Shao ^c, Yuxue Liu ^c, Changshan Xu ^c

^a Key Laboratory of Excited State Processes, Changchun Institute of Optics, Fine Mechanics and Physics, Chinese Academy of Sciences, Changchun 130033, People's Republic of China

^b Graduate University of Chinese Academy of Science, Beijing 100049, People's Republic of China

^c Centre for Advanced Optoelectronic Functional Material Research, Northeast Normal University, Changchun 130024, People's Republic of China

Received 3 April 2006; in final form 17 April 2006

Available online 26 April 2006

Abstract

ZnO hexagonal prisms have been successfully synthesized in large scale by microemulsion method with polyvinyl pyrrolidone (PVP) used as surfactant to form the template for the growth of ZnO and passivant for the modification of ZnO prisms surface, simultaneously. The as-prepared prisms show high crystal quality and Raman spectra indicate that the ZnO prisms are in wurtzite phase. In the presence of adsorbed PVP, the ZnO hexagonal prisms show an intensive near-band-edge emission. Our protocol provides an effective method to synthesize ZnO nanomaterials with perfect morphology, pure crystal quality and intensive UV emission.

© 2006 Elsevier B.V. All rights reserved.

1. Introduction

Recently, numerous researches have been focused on novel synthetic methodologies for well-controlled nanomaterials, including controlled size and shape, which are important for their chemical and physical properties. Among these materials, the II–VI *n*-type direct wide band-gap semiconductor ZnO, with a large exciton binding energy (60 meV), is considered to have possible applications in blue/ultraviolet (UV) optoelectronic devices and piezoelectric devices [1]. In addition, low dimensional ZnO nanomaterials, due to the quantum confinement effects, offer the possibility for further improving lasing conditions [2]. Therefore, preparing ZnO nanomaterials with controlled shape is a focus for chemists, physicists and material scientists.

Up to now, several physical and chemical methods have been demonstrated for the preparation of ZnO nano- and micro-structures with different morphologies [3–6]. How-

ever, these methods still have some disadvantages. For example, the physical methods require exacting experimental conditions, such as high vacuum or high temperature, which make them inconvenient for large-scale production [3,4]. While for the chemical methods, although cheap and flexible, contamination or defect is usually hard to avoid, this in turn deteriorates the photoluminescence and hinders the application of ZnO in optoelectronic and lasing devices [5,6]. Therefore, how to improve the crystal quality of ZnO and realize UV emission and lasing, are still major challenges.

Herein, we introduce a polyvinyl pyrrolidone (PVP) assisted microemulsion method to prepare ZnO hexagonal prisms in large scale with intensive UV photoluminescence. PVP has shown the surface modification for ZnO nanoparticles [7], while in our method, PVP molecules are employed as both passivants to quench the visible emission of ZnO and surfactants to form the template for the growth of ZnO. In the presence of PVP, the as-prepared ZnO hexagonal nanoprisms exhibit high crystal quality as well as the intensive near-band-edge UV photoluminescence.

* Corresponding author. Fax: +86 431 5684009.

E-mail address: ycliu@nenu.edu.cn (Y. Liu).

2. Experimental section

Firstly, 5 g PVP ($M_w = 30,000$) was dissolved in 7 ml 1-butanol under vigorously stirring, then the as-prepared PVP solution was added to an aqueous solution of $\text{Zn}(\text{NO}_3)_2 \cdot 6\text{H}_2\text{O}$ (0.025 M) to form a PVP microemulsion. The volume ratio of the aqueous phase to the organic phase was kept at 10:1. After stirred for 2 h, a concentrated aqueous solution of $\text{NH}_3 \cdot \text{H}_2\text{O}$ ($\text{NH}_3 \cdot \text{H}_2\text{O}:\text{Zn}(\text{NO}_3)_2 \cdot 6\text{H}_2\text{O} = 4$, molar ratio) was added dropwise to the microemulsion and kept stirring for another 3 h at room temperature. Subsequently, the resulted milky white mixture was kept at 75 °C for 5 days. Then the obtained white suspension was centrifuged to separate the precipitate, which was washed several times by distilled water and absolute ethanol to remove the un-adsorbed PVP molecules, sequentially. Finally, some white powder was obtained.

The surface morphology was investigated by a field-emission scanning electronic microscopy (FESEM) (XL 30 ESEM FEG SEM, FEI Company) and a transmission electron microscopy (TEM) (JEOL-JEM-2010, JEOL) with accelerate voltage of 200 kV. For FESEM measurement, the as-prepared sample was stick to the metal substrate by conductive rubber fabric without gold coating. Fourier transform infrared spectroscopy (FTIR) spectrum was obtained on Magna 560 FTIR spectrometer with resolution of 1 cm^{-1} . X-ray diffraction (XRD) pattern was recorded by a Siemens D5005 Diffractometer, scans were ranged from 25° to 70° (2θ) at the speed of 2° min^{-1} , using Ni-filtered $\text{CuK}\alpha$ line of 1.5418 \AA . Non-resonant Raman and photoluminescence (PL) measurement was performed on a HR-800 LabRam confocal Raman microscope made by JY Company, excited by the 488 nm line of an argon-ion laser and the 325 nm line of a continuous He–Cd laser at room temperature, respectively.

3. Results and discussion

The size and morphology of the samples were examined by FESEM. Fig. 1a shows the typical low-magnification SEM image of ZnO. The as-synthesized product is dominated by hexagonal prisms with uniform size and well-defined shape. Fig. 1b gives the high-magnification SEM image. The prisms show well-resolved edges and corners with smooth surfaces. The angle between the two adjacent edges of an individual prism is about 120° , average size of the side edge is about 500 nm and average height about 600 nm. Energy-dispersive X-ray spectroscopy (EDS) composition analysis (Fig. 1c) shows that only Zn and O signal were detected within experimental limits.

Fig. 1d shows the XRD pattern of the as-prepared ZnO nanoprisms. All the reflection peaks of the samples are indexed to pure hexagonal wurtzite structural ZnO, (JCPDS card number 36-1451). The full width at half maximum (FWHM) of (101) peak is only 0.07° , indicating super crystal quality. Because of low content and poor

crystal property of PVP, the semi-crystal diffraction peaks of PVP were not detected by the XRD characterization.

The typical TEM morphology of the samples is shown in Fig. 2, which shows the top and side view of the hexagonal prism. Insert is the corresponding selected area electron diffraction (SAED) pattern, indicating a single crystal structure, which consists with XRD result. The top view of the TEM images confirms the perfect hexagonal structure of the samples. While from the side view, top and bottom of the ZnO nanoprisms show different morphologies. The bottom surface of the prism is smooth, flat, and perfect, while the top side is coarse, convex and incomplete at the edge.

From the viewpoint of the molecular structures, the oxygen atom is more electronegative than nitrogen atom and it is expected that the negative charge on PVP prefers to reside on oxygen atom. The partial positive charge on the nitrogen atom and the partial negative charge on the oxygen atom can behave as electron acceptor and donor, respectively [8,9]. Hence, the PVP molecules may exist in two resonance structures as shown in the Scheme 1. In polar circumstance, such as in water, the inner molecular acylamino bond (a) is intent to transform to hydrophilic $-\text{N}^+=\text{C}-\text{O}^-$ bond (b). Together with the hydrophilic $\text{C}-\text{O}^-$ bond, the hydrophobic $\text{C}-\text{C}$ bond makes the PVP an alternate surfactant. The atom N locates inner the PVP molecule and has a saturated covalent bond, while the atom O locates outside of the molecule, thus PVP shows more anionic properties. The PVP can be made to form micelles by adjusting experimental parameters. The self-assembled PVP layers at the interface of water and oil can act as template for the growth of ZnO. The hydrophilic head of PVP is supposed to be exposed to water, and thus Zn^{2+} cation can directly attach to the negatively charged $\text{C}-\text{O}^-$ group of PVP template to initiate the first layer of crystal growth. By reaction with $\text{NH}_3 \cdot \text{H}_2\text{O}$ and hydration at high experiment temperature, the positively charged Zn^{2+} is transformed to the surface of ZnO. Due to electrostatic interaction, a number of alternating planes composed of tetrahedral coordinated O^{2-} and Zn^{2+} ions stacks alternatively along the c axis.

The growth mechanism of such morphology with different top and bottom surface is quite similar to the growth mechanism proposed by Li et al. [10]. According to Li, the Zn^{2+} surface bonds strongly to PVP due to charge interaction, and the densely packed PVP will protect the surface from further ‘etching’ or reaction, resulting in the formation of the flat side of the prism. The PVP template stabilizes the surface charge and the structure. While in the absence of PVP, the exposed negatively charged O^{2-} surface of the prism may react with NH_4^+ , then forming the rougher surface.

In order to prove the existence of PVP in the as-prepared sample, FTIR spectrum was applied, as shown in Fig. 3. In the spectrum of PVP molecule (Fig. 3a), the peaks labeled by number located at 3450, 2930, 1675, 1420, and 1290 cm^{-1} , are assigned to the O–H stretching

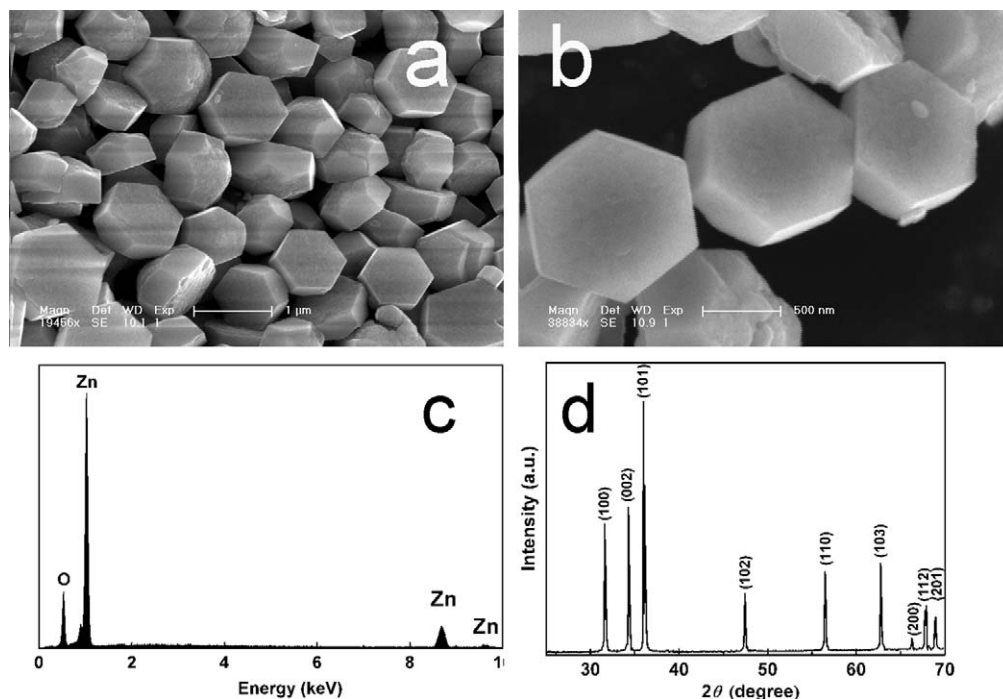


Fig. 1. Low magnification scanning electron micrograph image recorded from the as-prepared ZnO hexagonal prisms grown in PVP microemulsion (a). Enlarged image display detailed structures of the prisms (b). Energy-dispersive X-ray spectroscopy of the sample and (c). X-ray diffraction pattern of wurtzite ZnO hexagonal prisms with a high degree of crystallinity (d).

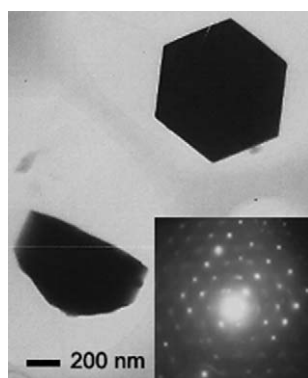
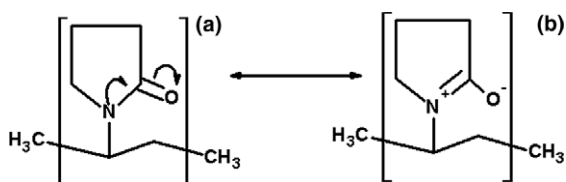


Fig. 2. Transmission electron micrograph image of top-view and side-view of PVP-assisted ZnO hexagonal prisms and corresponding selected area electron diffraction pattern inserted.



Scheme 1. Schematic of the resonance structures of PVP molecule.

vibration, CH_2 unsymmetrical stretching vibration, $\text{C}=\text{O}$ stretching vibration, CH_2 bending vibration and $\text{C}-\text{N}$ stretching vibration band, respectively. The intensive and sharp vibration band of $\text{C}=\text{O}$ indicates that the structure in Scheme 1a is the dominant structure. In the FTIR spec-

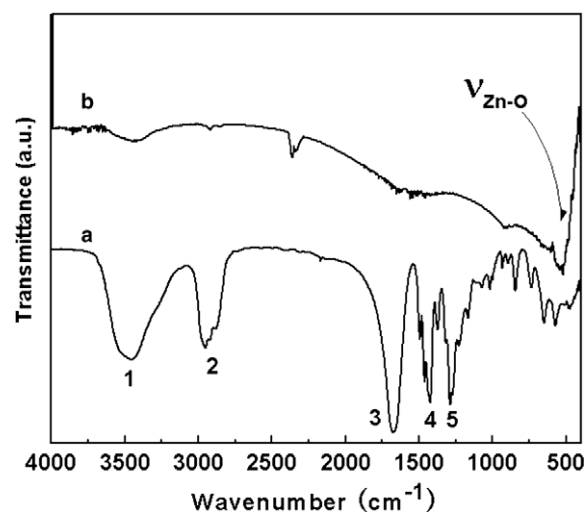


Fig. 3. FT-IR spectra of PVP molecules (a) and PVP-assisted ZnO hexagonal prisms (b). The peaks labeled numerically are assigned to the O-H stretching vibration, $-\text{CH}_2-$ stretching vibration, $\text{C}=\text{O}$ stretching vibration, CH_2 bending vibration and $\text{C}-\text{N}$ stretching vibration band of PVP, respectively. The arrow indicates the stretching vibration of $\text{Zn}-\text{O}$ bond.

trum of ZnO hexagonal prisms (Fig. 3b), the most intensive sharp band in the vicinity of $460\text{--}500\text{ cm}^{-1}$ is assigned to the $\text{Zn}-\text{O}$ vibration [11]. Besides the vibration band of $\text{Zn}-\text{O}$ bond, the strong sharp vibration band of $\text{C}=\text{O}$ is replaced by a weak and broad band located from 1400 to 1700 cm^{-1} which is considered to be combined of the stretching vibration band of PVP molecule's $\text{C}=\text{O}$ group

and resonant structure $>\text{N}^+=\text{C}-\text{O}^-$ [12,13]. The C–N stretching vibration band is hard to be observed, indicating the structure (b) is the dominant structure under the interaction of Zn^{2+} and C–O $^-$ group of PVP. The intensity of the O–H stretching vibration, CH_2 symmetrical and unsymmetrical stretching vibration of the sample become weak evidently compared to that of PVP molecules, which may be caused by the low content of PVP absorbed on the surface of ZnO prisms. The FTIR results indicate that there remain chemical absorbed PVP molecules on ZnO nanoprisms. It is expected that PVP molecules absorbed on the surface of ZnO prisms may influence the optics properties of ZnO.

Fig. 4 shows the Raman spectrum of the sample. Wurtzite ZnO belongs to the C_{6v}^4 space group ($\text{P6}_3\text{mc}$). At the Γ point of the Brillouin zone, the normal lattice vibration modes are predicted on the basis of group theory: $\Gamma_{\text{opt}} = A_1(z) + 2B_1 + E_1(x, y) + 2E_2$ [14,15]. Among these, E_1 , E_2 , and A_1 are the first-order Raman active modes. E_1 and A_1 are also infrared active. B_1 is forbidden. In bulk ZnO, generally, only E_2 and the A_1 (LO) modes can be observed in unpolarized Raman spectra taken in backscattering geometry according to the well-known selection rules. The band at 378 cm^{-1} corresponds to A_1 symmetry with the TO mode. The bands at 408 and 583 cm^{-1} are E_1 symmetry with TO and LO modes, respectively. The band at 436 cm^{-1} is attributed to ZnO nonpolar optical phonons high E_2 vibration mode, which correspond to the characteristic band of wurtzite phase with high crystal quality. The Raman results confirm the conclusion drawn from the former discussion.

Fig. 5 shows the PL spectrum of the ZnO hexagonal nanoprisms. PVP has a neglectable emission band under the 325 nm line of He–Cd laser. The typical PL spectrum of ZnO usually exhibits two emission bands located at about 370 and 550 nm, respectively. The emission band

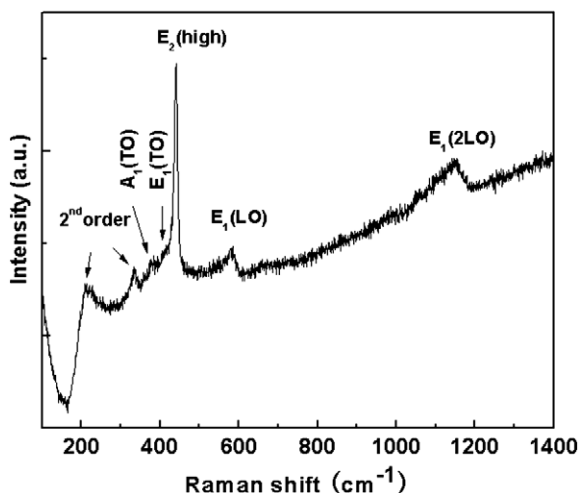


Fig. 4. Raman spectrum of ZnO hexagonal nanoprism. The band at 436 cm^{-1} is attributed to ZnO nonpolar optical phonons high E_2 vibration mode, which correspond to the wurtzite phase with high crystal quality.

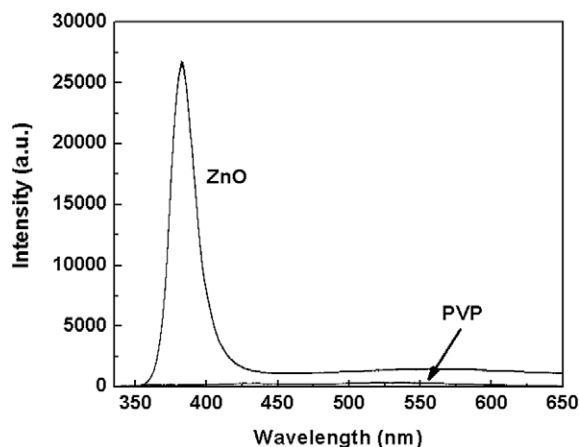


Fig. 5. Photoluminescence spectra of ZnO hexagonal prisms and PVP. At the passivation effect of PVP molecules adsorbed on the surface, the ZnO prisms exhibit intensive UV near-band-edge photoluminescence.

at about 370 nm is typically originated from the exciton combination of ZnO [16,17], and can be attributed to UV near-band edge emission. The green emission at about 550 nm is the transition between the electron close the conduction band and deeply trapped hole at V_{O}^{**} centre (oxygen vacancy containing no electrons) [18,19], which is also attributed to the transition between the electron at $[V_{\text{O}}^*, \text{electron}]$ or $[V_{\text{O}}^{**}, \text{two electrons}]$ and the hole at vacancy associated with the surface defects [20]. Due to the poor crystal quality of ZnO synthesized by other chemical methods, the UV emission of ZnO is liable to be quenched and only defect-related emission in visible region is detected [5].

By the addition of PVP, the PL spectrum of ZnO prisms shows an intensive UV emission and the visible emission is quenched. The PL intensity ratio of the UV band-edge emission to the deep-level green emissions ($I_{\text{U}}/I_{\text{D}}$), which can be used to estimate the relative density of defects, is drastically high. In terms of experimental results, two reasons are supposed to contribute to the high $I_{\text{U}}/I_{\text{D}}$ ratio. One is that the crystal quality of the as-prepared sample is enhanced by reducing the density of defects inside the crystals during the growing of ZnO prisms. The second reason is that PVP molecules adsorbed onto the surface of prisms decrease the density of oxygen vacancy sites on ZnO facets. These two effects prevent the formation of V_{O}^{**} to decrease the recombination centers of visible emission, and thereby decreasing the intensity of the visible emission.

4. Conclusion

In summary, a microemulsion method has been developed for the growth of ZnO hexagonal prisms with PVP serving as surfactant and passivant. The as-prepared ZnO hexagonal prisms exhibit perfect morphology and high crystal quality. The PVP-assisted ZnO prisms show enhanced near-band-edge UV emission and reduced

defect-relate green emission. In general, under certain modification, the method reported in this article can be applicable for preparation of many other oxides, carbides, nitrides, etc., with both good morphology and optic properties.

Acknowledgements

This work was supported by the National Natural Science Foundation of China (60376009), the Cultivation Fund of the Key Scientific and Technical Innovation Project, Ministry of Education of China (704017), the Key Project of the Chinese Ministry of Education (104071), and the Science Foundation for Young Teachers of Northeast Normal University (20050301).

References

- [1] C.X. Xu, X.W. Sun, B.J. Chen, P. Shum, S. Li, X. Hu, *J. Appl. Phys.* 95 (2004) 661.
- [2] P. Yang, H. Yan, S. Mao, R. Russo, J. Johnson, R. Saykally, N. Morris, J. Pham, R. He, H. Choi, *Adv. Funct. Mater.* 12 (2002) 323.
- [3] M.H. Huang, S. Mao, H. Feick, H. Yan, Y. Wu, H. Kind, E. Weber, R. Russo, P. Yang, *Science* 292 (2001) 1897.
- [4] J.Y. Lao, J.Y. Huang, D.Z. Wang, Z.F. Ren, *Nano Lett.* 3 (2003) 235.
- [5] M. Yin, Y. Gu, I.L. Kuskovsky, T. Andelman, Y. Zhu, G.F. Neumark, S. O'Brien, *J. Am. Chem. Soc.* 126 (2004) 6206.
- [6] J. Zhang, L. Sun, J. Yin, H. Su, C. Liao, C. Yan, *Chem. Mater.* 14 (2002) 4172.
- [7] L. Guo, S. Yang, C. Yang, P. Yu, J. Wang, W. Ge, G.K.L. Wong, *Appl. Phys. Lett.* 76 (2000) 2901.
- [8] M.M. Robert, M.K. Jonathan, *Tetrahedron Lett.* (1966) 891.
- [9] M.C.R. Symons, J.M. Harvey, S.E. Jackson, *J. Chem. Soc., Faraday Trans. 1* 76 (1980) 256.
- [10] F. Li, Y. Ding, P. Gao, X. Xin, Z.L. Wang, *Angew. Chem., Int. Ed.* 43 (2004) 5238.
- [11] S.C. Liufu, H.N. Xiao, Y.P. Li, *Polym. Degrad. Stab.* 87 (2005) 103.
- [12] H. Muta, K. Ishida, E. Tamaki, M. Satoh, *Polymer* 43 (2002) 103.
- [13] A. Drelinkiewicz, M. Hasik, S. Quillard, C. Paluszkiwicz, *J. Mol. Struct.* 511–512 (1999) 205.
- [14] A. Kaschner, U. Haboeck, M. Strassbureg, G. Kaczmarczyk, A. Hoffmann, C. Thomsen, A. Zeuner, H.R. Alves, D.M. Hoffmann, B.K. Meyer, *Appl. Phys. Lett.* 80 (2002) 1909.
- [15] T.C. Damen, S.P.S. Porto, B. Tell, *Phys. Rev.* 142 (1966) 570.
- [16] P. Yu, Z.K. Tang, G.K.L. Wong, M. Kawasaki, A. Ohtomo, H. Koinuma, Y. Segawa, *J. Cryst. Growth* 184 (1998) 601.
- [17] J.F. Scott, *Phys. Rev. B* 2 (1970) 1209.
- [18] A. van Dijken, E. Meulenkamp, D. Vanmaekelbergh, A. Meijerink, *J. Phys. Chem. B* 104 (2000) 1715.
- [19] A. wood, M. Giersig, M. Hilgendorff, A.V. Campos, L.M. Lizmarzan, P. Mulvaney, *Aust. J. Chem.* 56 (2003) 1051.
- [20] Y.C. Liu, X.T. Zhang, J.Y. Zhang, Y.M. Lu, X.G. Kong, D.Z. Shen, X.W. Fan, *Chin. J. Lumin.* 23 (2002) 563.